



PDF hosted at the Radboud Repository of the Radboud University Nijmegen

The following full text is a publisher's version.

For additional information about this publication click this link.

<http://hdl.handle.net/2066/115536>

Please be advised that this information was generated on 2017-12-05 and may be subject to change.

Optical imaging of trion diffusion and drift in GaAs quantum wells

F. Pulizzi,^{1,*} D. Sanvitto,^{2,3,†} P.C.M. Christianen,¹ A.J. Shields,² S.N. Holmes,² M.Y. Simmons,^{3,‡} D.A. Ritchie,³ M. Pepper,^{2,3} and J.C. Maan¹

¹*Research Institute for Materials, High Field Magnet Laboratory, University of Nijmegen, Toernooiveld 1, 6525 ED Nijmegen, The Netherlands*

²*Toshiba Research Europe Limited, Cambridge Research Laboratory, 260 Cambridge Science Park, Milton Road, Cambridge CB4 0WE, United Kingdom*

³*Cavendish Laboratory, University of Cambridge, Madingley Road, Cambridge CB3 0HE, United Kingdom*

(Received 29 January 2003; revised manuscript received 24 June 2003; published 7 November 2003)

The in-plane motion of negatively charged excitons (X^-) in modulation-doped GaAs quantum wells (QW's) was studied by means of spatially resolved photoluminescence spectroscopy. In the highest-quality QW's, resonantly excited X^- were observed diffusing from the excitation region, characterized by a mobility as high as $6.5 \times 10^4 \text{ cm}^2 \text{ V}^{-1} \text{ s}^{-1}$, independent of temperature and electron density. Under the application of an electric field in the plane of the QW, X^- were found to drift in the direction opposite to the field, whereas neutral excitons (X) do not drift under similar conditions. The results demonstrate that X^- can exist as a free quasiparticle in the best-quality samples. The simultaneous motion of nonresonantly excited X and X^- was studied as a function of the electron density in the QW. The data reveal that the spatial distribution of X and X^- is mainly determined by the motion of X that locally form X^- .

DOI: 10.1103/PhysRevB.68.205304

PACS number(s): 71.35.Pq, 78.55.Cr, 71.35.-y

I. INTRODUCTION

The optical properties of semiconductor heterostructures are dominated by excitonic resonances. For example, the exciton (X), a Coloumb-bound electron-hole pair, is the first excited state of an undoped structure and is often regarded as the semiconductor analog of the hydrogen atom. If a low concentration of extra charges is present in the material, such a charge can be captured by a photoexcited exciton to form a new three-particle complex—i.e., a charged exciton or, more simply, a trion.¹ According to the sign of the extra charge, the trion is either negatively (X^-) or positively (X^+) charged, which can be seen as the analog of the negative hydrogen ion (H^-) or of the positive hydrogen molecule (H_2^+), respectively. As the binding energy of the extra charge is quite small in bulk materials, unambiguous proof of the existence of trions was only obtained after the advent of high-quality remotely doped quantum well (QW) structures, in which the confinement along the growth direction considerably enhances the binding energy of excitonic complexes. Soon after the first observation of negative trions in CdTe-based QW's,² both negative^{3–5} and positive^{4,5} trions have been observed in several material systems.

These charged complexes composed of a few particles have attracted a considerable amount of research interest in recent years, because they provide a model system to study electron-electron interactions in quantum systems. H^- has been studied for many years in this regard.⁶ Compared to H^- , X^- offers some advantages, such as the possibility to study electron-electron interactions in two-, one-, and zero-dimensional systems. Moreover, the binding energy of X^- is much smaller than that of H^- , which implies that the effect of external fields can be studied experimentally. In particular, the possibility to study the effect of an external magnetic field has allowed the investigation of issues that could not be investigated for H^- , since this would require field strengths

much higher than those available. For example the so-called spin-triplet state of X^- , in which the two constituent electrons have parallel spin, has been observed in magnetophotoluminescence (PL) spectra,^{7,8} and new lines in the reflectivity and photoluminescence-excitation (PLE) spectra of a two-dimensional electron gas of low density in a magnetic field have been attributed to combined exciton-cyclotron resonances.⁹

Since the first experimental observation, there has been a considerable debate whether negative trions can exist as mobile, free quasiparticles. According to several experimental studies,^{10,11} charged excitons are trapped in potential fluctuations generated by doping ions, introduced in the barrier layer to provide extra charges in the QW layer. In this case the trion is bound to a barrier donor and cannot be considered as an independent entity formed by three charged particles. On the other hand, circumstantial evidence has been found for the existence of free negative trions, such as the linear temperature dependence of the radiative lifetime^{12,13} as predicted for free particles.¹⁴ The question is of considerable importance in order to build and test a theoretical model for this three-body system. In addition, the observation of free trions and the ability to detect their motion opens the way for more extended investigations of their physical properties.

Following the suggestion of Stébé and co-authors,¹⁵ we have recently demonstrated the existence of free negative trions by observing their drift in an external electric field.¹⁶ The trions were excited in a very small area and their spatial distribution in the QW plane was monitored by a new continuous-wave (cw) PL imaging technique. Compared to other, mainly time-resolved methods,^{17,18} this technique offers several advantages. First of all, it provides direct, intuitive PL images in real space that are relatively easy to interpret. Second, since it is a cw technique, it is very well suited to reach very low excitation intensities where spurious effects of the illumination are kept to a minimum and the trans-

port of single excitonic complexes can be measured. In this paper we report an extended investigation of the trion diffusion and drift based on the same experimental technique. We show that negatively charged excitons can be treated as free, negatively charged quasiparticles, and their motion can be described by classical diffusion and drift in electric field. Also in the absence of external forces trions diffuse away from the excitation spot and their diffusion constant, or mobility, can be determined using a simple diffusion model. Using the same mobility we simulate the trion drift in applied in-plane electric field and find a good agreement with the corresponding experimental results. It is important to note that the significance of these results goes beyond the mere clarification of the controversy on the localization properties of X^- : they open the way to a new type of experiments, which involve the transport properties of X^- , an issue that is basically unexplored, both experimentally and theoretically. For instance, measuring the trion transport as a function of the concentration of excess electrons provides a direct method to investigate the electron-trion scattering. Furthermore, application of a magnetic field will allow studying and comparing the transport properties of singlet and triplet states.

The diffusion of trions has previously been reported as the result of space- and time-resolved PL in an experiment in which both excitons and trions were formed from the relaxation of photoexcited free electron-hole pairs.¹⁸ Here we will show that under such conditions it is very difficult to study the trion motion independently of that of the excitons,¹⁹ by using nonresonant excitation and monitoring the simultaneous motion of excitons and trions as a function of the concentration of extra electrons present in the sample.

The paper is organized as follows: in Sec. II we describe the samples studied and the optical setup used. In Sec. III we report our experimental data: the effect of the variation of electron density on the PL spectra, the diffusion and drift experiments of resonantly excited trions under varying experimental conditions, and the simultaneous motion of excitons and trions after nonresonant excitation. In Sec. IV we present a simple diffusion-drift model, which allows us to determine the trion mobility and its dependence on temperature and electron density. In Sec. V we apply the diffusion model to the simultaneous motion of neutral and charged excitons, showing the important influence of the exciton motion on the trion spatial distribution of the PL. All the experimental findings and their implications are summarized in Sec. VI.

II. EXPERIMENTAL DETAILS

The samples we have studied are two remotely doped GaAs/Al_{0.33}Ga_{0.77}As QWs, respectively 300 Å and 100 Å thick, grown by molecular beam epitaxy on GaAs substrates. The QW's are capped by a 600-Å-thick undoped Al_{0.33}Ga_{0.77}As spacer layer and a 2000-Å-thick Al_{0.33}Ga_{0.77}As layer doped with Si (10^{17} cm⁻³). The excess electron density can be controlled by applying a voltage between the Schottky NiCr gate (~ 4 mm²) evaporated on the top surface of the sample and an Ohmic contact to the QW

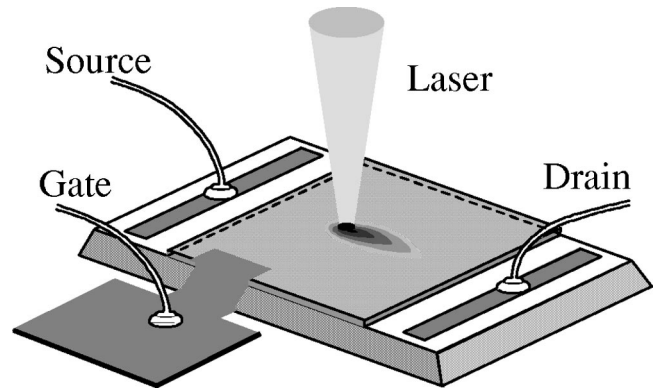


FIG. 1. Sketch of the experimental arrangement. Application of a voltage between gate and either source or drain allows us to change the electron density in the QW. Independently, a voltage applied between source and drain allow us to apply an electric field on the trions excited by the focused laser beam.

layer (Fig. 1). Furthermore, two Ohmic contacts (source and drain placed at 2 mm distance) to the QW layer allows us to apply an in-plane electric field, independently of the electron density in the QW. Time-resolved results obtained on these samples are reported in Ref. 12.

The samples are mounted in optical insert and placed in a He flow cryostat in which the temperature can be varied from 4.2 K to 300 K.

The beam of a cw tuneable Ti:sapphire laser is guided through a spatial filter to ensure a Gaussian intensity distribution and to set its divergence (via the positioning of the second lens). A 40 \times microscope objective focuses the laser beam to a 1.6- μ m-diam spot on the sample surface and collects the PL emission. The emission is guided through a monochromator and detected by a charge-coupled device (CCD) camera. By this method the image on the CCD camera is spectrally resolved along one of its axes and spatially resolved along the other (resolution 0.8 μ m). By taking the cross section at a particular spatial point we obtain the local PL spectrum. Equivalently, the cross section for a given emission energy gives the spatial profile of the PL.

All the data have been obtained with a constant laser power corresponding to an estimated concentration of excited electron-hole pairs of 10^9 cm⁻². In the case of resonant excitation at the X^- absorption line, we have filtered out the laser by inserting a polarizer in the excitation path and an analyzer in the detection path, placed in crossed configuration. Consequently, the detected laser intensity was comparable to the signal. The final image of the PL was obtained by the following procedure: first the image of the PL and laser light was measured at the desired gate voltage conditions. Second, the reflected laser light was recorded by acquiring an image without applied voltage, when the PL emission is both low in intensity and shifted towards lower energies with respect to the X^- peak (see Sec. III). Subtracting the two images resulted in a background-free PL emission profile.

III. EXPERIMENTAL RESULTS

A. Effect of gate voltage on the PL spectrum

The shape of the PL spectrum is directly related to the electron density tuned by the application of a gate voltage.³ A

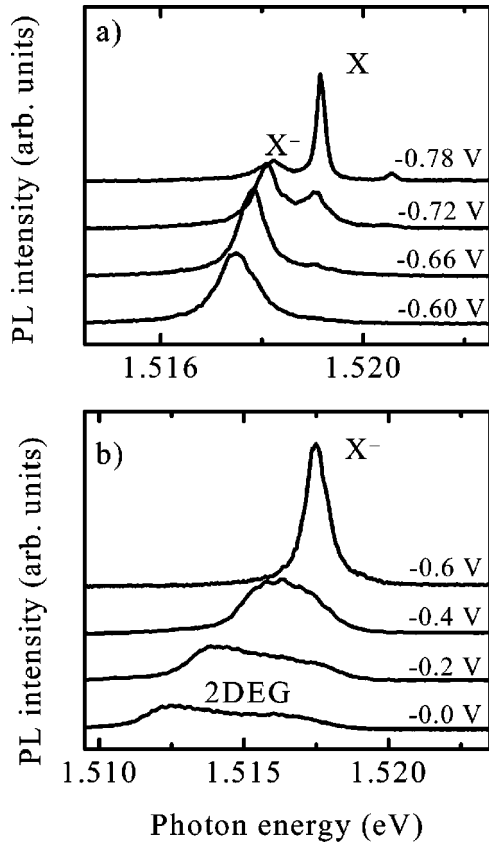


FIG. 2. Evolution of the PL spectrum with gate voltage for the 300-Å GaAs QW. The total voltage range has been split in two for clarity. Note the two different scales along the x axes of the two panels.

typical dependence is plotted in Fig. 2 for the 300-Å QW, measured at 4.2 K, using a (nonresonant) excitation energy of 1.6 eV. For very low applied gate voltage (< -0.78 V) almost no electrons are present in the QW and the PL spectrum shows a pronounced X peak at 1.519 eV. Upon increasing the gate voltage the electron density increases, resulting in a diminishing X peak and a simultaneous enhancement of the X^- PL intensity. Around a gate voltage of -0.62 V, corresponding to an electron density of $2 \times 10^{10} \text{ cm}^{-2}$,²⁰ the X PL is quenched and only X^- PL can be observed [Fig. 2(a)]. With further increasing gate voltage [Fig. 2(b)] the X^- peak merges into a broad feature that is the signature of a two-dimensional electron gas (2DEG). For zero applied gate voltage, the concentration of the photoexcited electron-hole pairs is much lower than that of the extra electrons in the QW. In this case the photoexcited electrons can be neglected and the PL emission is given by the recombination of the 2DEG with the photoexcited holes. In fact, the width of the PL spectrum (1.5113–1.5175 eV) extends from the band gap energy to the Fermi edge, leading to an estimated Fermi energy of 4.3 meV and an electron concentration of $n_e = 1.2 \times 10^{11} \text{ cm}^{-2}$.²¹

B. Trion diffusion after resonant excitation

In order to study the motion of negatively charged excitons avoiding the effect of neutral excitons, the laser energy

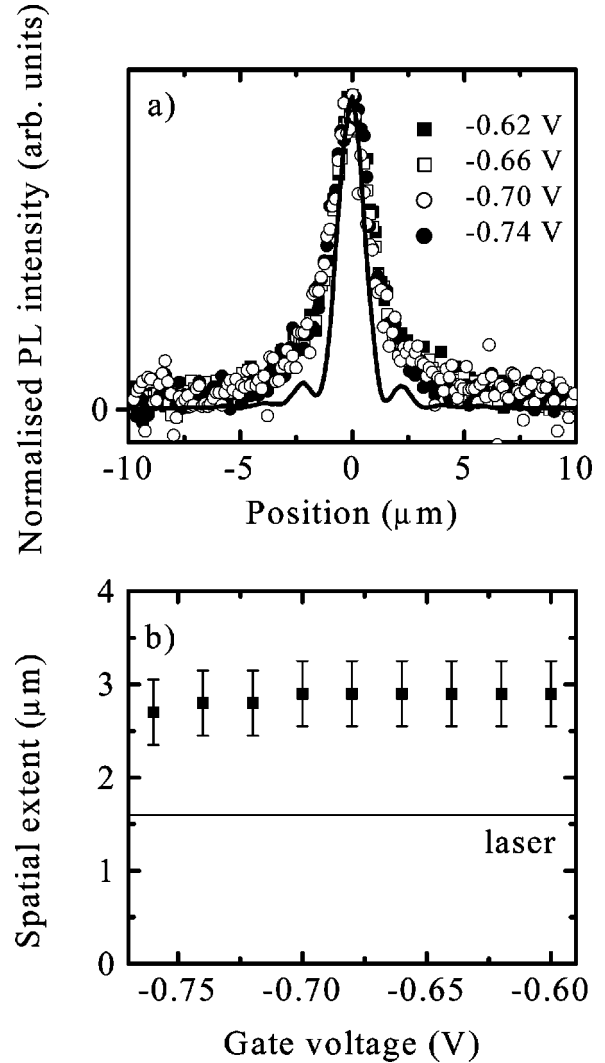


FIG. 3. (a) Spatial profiles of the X^- PL emission after resonant excitation as a function of the gate voltage. The solid line is the laser profile. (b) Spatial extent of the PL intensity (symbols) as a function of gate voltage. The solid line is the spatial extent of the laser. The data have been recorded from the 300-Å QW at 4.2 K.

was tuned to quasiresonance with the X^- absorption peak—that is, at its high-energy wing (1.5183 eV)—below the X resonance. At low temperatures (< 8 K) the energy splitting between the X and X^- peaks (~ 1 meV) is large enough to prevent excitation of X .^{22,23}

Experimental evidence for diffusion of X^- is shown in Fig. 3, which compares the spatial profile of the 300-Å QW PL to the laser excitation profile in the whole gate voltage range at which the X^- peak can be observed. For gate voltages lower than -0.76 V, the X^- peak is too weak to collect an image under resonant excitation conditions. Figure 3(a) shows that the PL profile is always larger than the laser profile, demonstrating that trions diffuse away from their point of excitation.

In order to quantify the X^- motion we have defined the spatial extent of the PL profiles as the full width at $1/e$ of the PL intensity maximum. As shown in Fig. 3(b) decreasing the gate voltage has only a very small effect (within the spatial

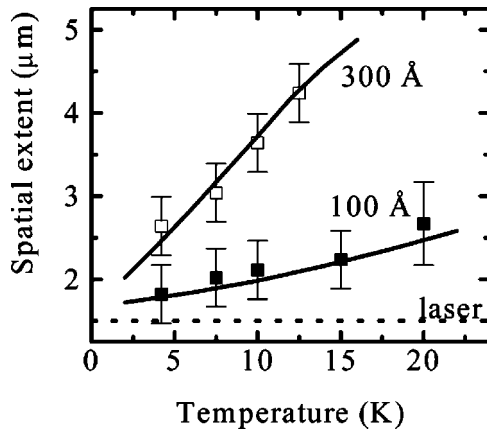


FIG. 4. Temperature dependence of the spatial extent of the X^- PL profile in the 300-Å and 100-Å QW's without in-plane electric field. The solid lines correspond to the calculated results of the diffusion model, assuming a temperature-independent X^- mobility.

resolution) on the spatial extent of the PL. This result shows that, in this range of electron densities, trions are able to move in the QW plane and that their motion does not depend on the electron density; i.e., the trion transport seems not substantially affected by scattering with electrons.

The X^- motion has been measured for both samples as a function of temperature. For each temperature the gate voltage has been set to the value at which only the X^- peak is visible in the PL spectrum. This reduces possible effects of thermal excitation of X . For both samples the profile broadens with temperature, although at the lowest temperature their behavior differs.¹⁶ In the case of the 300-Å QW the profile is always evidently larger than the laser spot, meaning that X^- is free and mobile at all temperatures measured. In the 100-Å sample we find that at 4.2 K the PL profile coincides with the laser within the resolution of the optical setup, in agreement with X^- localization as expected for this sample at 4.2 K, from time-resolved experiments.¹² However, at higher temperatures the PL profile becomes larger than the laser profile, showing the ability of X^- to move also in this sample. The measurements are summarized in Fig. 4, which displays the spatial extents of the measured spatial profiles (symbols), together with the calculated results of a simple diffusion model (solid lines), explained in Sec. IV.

C. Trion drift in electric field

An alternative method to illustrate the ability of trions to move in the QW plane is the observation of their drift in an electric field. Therefore we have imaged the PL distribution of X^- after pointlike resonant excitation in the presence of an in-plane voltage.

Figure 5(a) shows the PL profiles for the 300-Å QW, recorded at 4.2 K and at a gate voltage of -0.62 V, where only the trion peak is visible in the PL spectrum. Under the influence of the in-plane voltage the PL profile is skewed in the direction opposite to that of the electric field. The asymmetry increases with increasing in-plane voltage, and the profile flips along the spatial axis after reversing the field. These results provide a strong confirmation that in this

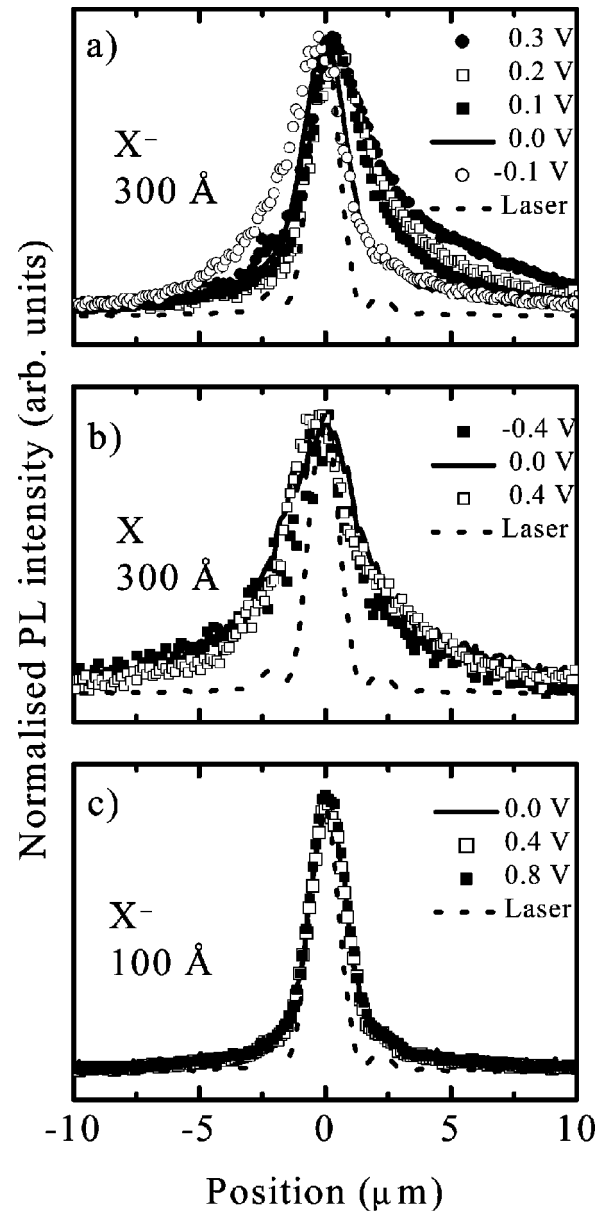


FIG. 5. Spatial profiles of the PL emission at 4.2 K after application of an in-plane voltage (a) X^- profiles for the 300-Å QW, (b) X profile for the 300-Å QW, and (c) X^- profiles for the 100-Å QW.

sample trions behave as free negatively charged quasiparticles which drift in an applied electric field. It is important to note that these results can only be explained by trion transport and not by transport of holes, which would be directed along the applied field or by transport of neutral excitons. Since the trions are photoexcited resonantly, no exciton PL is visible, even at the highest value of the in-plane voltage. As a consequence, the possible mechanism that the trion dissociates into an exciton and an electron, then the exciton moves out of the excitation spot (either due to diffusion or due to drag by electrons), to form a new trion elsewhere where it recombines, is very unlikely. Namely, in that case an appreciable amount of exciton PL should be visible. In addition, we have verified experimentally that the exciton is not sensitive to the electric field and therefore cannot explain the

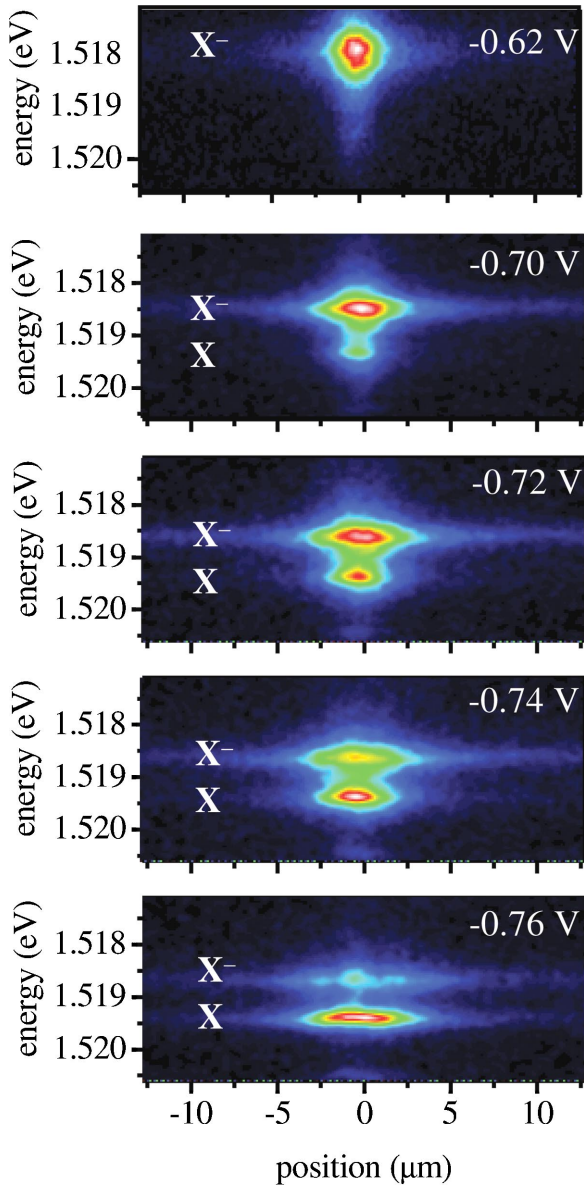


FIG. 6. (Color online) Spectrally and spatially resolved images of the PL emission from X and X^- in the case of nonresonant excitation (at 1.6 eV) for various gate voltages.

specific field dependence depicted in Fig. 5(a). The PL profiles in Fig. 5(b) are recorded at a gate voltage of -0.75 V, where X dominates the spectrum, using an excitation energy of 1.5193 eV—i.e., on the high-energy wing of the X absorption peak. Indeed, without in-plane voltage the exciton profile is larger than the laser spot and the trion profile, which indicates efficient exciton transport. However, the width of the exciton profile is essentially independent of the value of the applied in-plane field, as expected for a neutral particle.

Finally, further confirmation is given by the different behavior of the 100-Å sample at 4.2 K [Fig. 5(c)] where the trions are believed to be localized (Sec. III B). Irrespective of the in-plane electric field the PL profile coincides with the laser. The lower quality of this sample is attributed to an

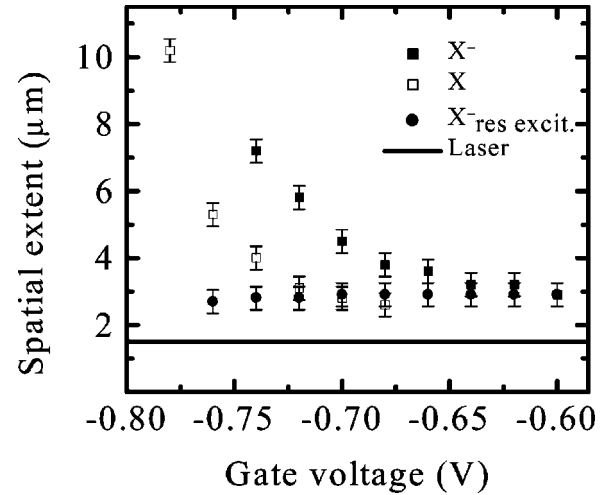


FIG. 7. Width of the PL spatial profile for excitons (open squares) and trions (solid squares) of the 300-Å QW at 4.2 K as a function of the gate voltage. The excitation energy was fixed at 1.6 eV (nonresonant excitation). The solid circles correspond to the results of X^- after resonant excitation. The solid line is the spatial extent of the laser profile.

increased interface roughness that considerably limits the motion of excitonic complexes.^{24,25}

D. Nonresonant excitation

In order to study the effect of the electron density on the simultaneous motion of X and X^- , we have recorded the PL images after pointlike excitation at 4.2 K as a function of the gate voltage, with an excitation energy fixed at 1.6 eV.

As we have mentioned in Sec. II A, under nonresonant excitation, the PL spectrum shows peaks due to both the neutral and charged excitons, with relative intensities depending on the gate voltage applied. In general it can be seen that the X^- profile is much wider than under resonant excitation and that the width of both profiles decreases with increasing electron density (see Fig. 6).

At the most negative applied gate voltage (-0.76 V) in Fig. 6, the PL is dominated by recombination of X with a much weaker feature at lower energy due to X^- . The X PL shows a smoothly decreasing intensity away from the laser spot. The much weaker X^- PL has a similar spatial extent to that of X , but shows a nonmonotonic variation in intensity with position. Similar behavior has been observed in near-field scanning optical microscope experiments.¹¹ We attribute this behavior to the localization of the excess electrons into puddles at the most negative gate bias. This is consistent with the 2DEG being highly resistive at these biases. The profile does not change at higher negative biases because the applied bias is dropped across the highly resistive Ohmic contacts. As discussed below, under nonresonant excitation conditions and low excess electron densities the profiles are dominated by diffusion of the neutral excitons. Thus we observe PL from X^- over a wide spatial region due to the diffusion of X followed by X^- formation. At the most nega-

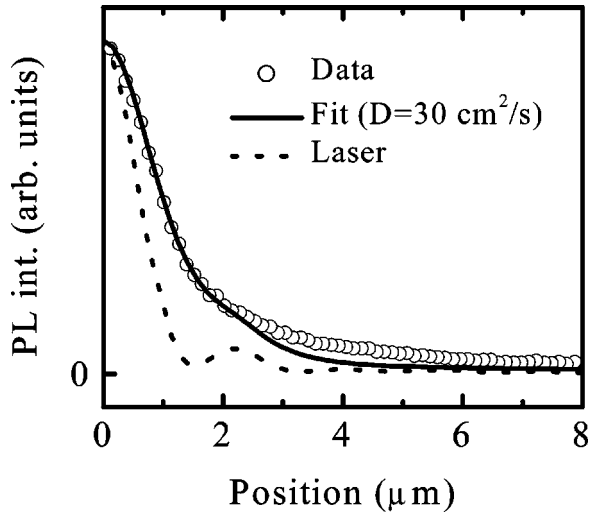


FIG. 8. Result of the fitting procedure of the PL profile of X^- for the 300-Å QW at 4.2 K using the diffusion equation (2).

tive gate voltage this occurs only in the regions of the electron puddles leading to the irregularities in the X^- spatial profile.

Figure 7 summarizes the results of the experiment and displays the spatial extent for both excitonic complexes as a function of the gate voltage. For comparison also the spatial extent for the X^- in the case of resonant excitation is plotted [Fig. 3(b)]. For very low gate voltage (-0.78 V) the trion peak is barely visible and cannot be measured. The same holds for the X peak at a gate voltage larger than -0.70 V. The two excitation conditions (resonant and nonresonant) clearly show different behavior. For resonant excitation the X^- extent stays constant with applied gate voltage, as shown in Figs. 3 and 7. On the contrary, for nonresonant excitation the spatial extent decreases for both species with increasing bias voltage and, in the case of trions, it tends to that observed for resonant excitation. A remarkable observation is the larger extent of the X^- PL, also observed in CdTe QW's,¹⁹ which we ascribe to a local variation of the X^- formation rate (see end of Sec. V).

IV. ANALYSIS AND DISCUSSION

The simplest way to describe the diffusion or drift of a population of mobile particles is given by the diffusion equation

$$D\nabla^2 n(x,y) + \mu \mathbf{F} \cdot \nabla n(x,y) + I(x,y) - \frac{n(x,y)}{\tau} = \frac{\partial n}{\partial t}, \quad (1)$$

where D is the diffusion constant, $n(x,y)$ is the local concentration of particles, μ is their mobility, \mathbf{F} is the external force, $I(x,y)$ is the injection profile of the particles, and τ is their lifetime. Our experiment uses cw laser excitation, and therefore it measures the steady-state solution of Eq. (1) with $\partial n / \partial t = 0$.

The diffusion equation can be applied whenever the particle distribution in velocity does not depend on the position

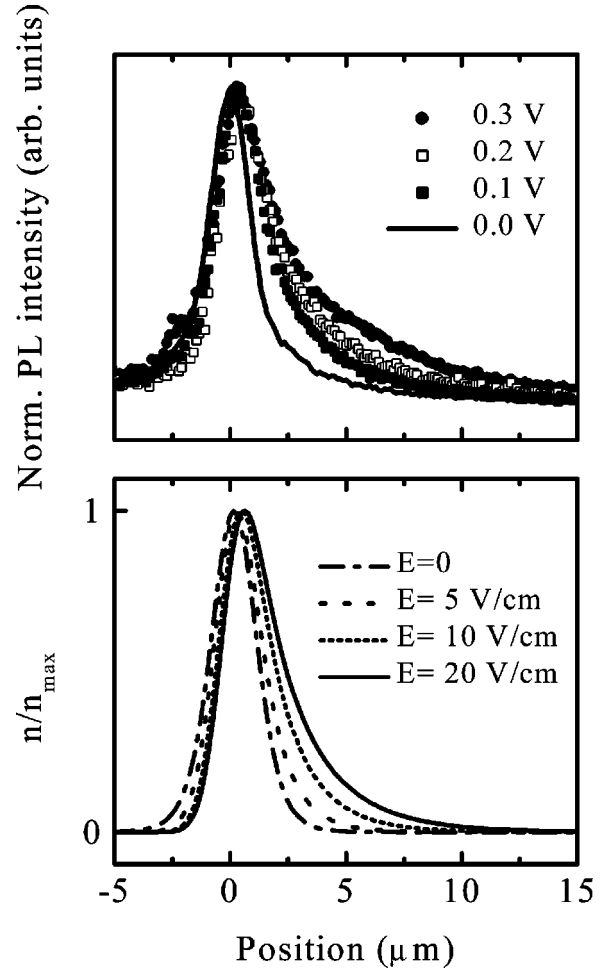


FIG. 9. X^- diffusion and drift as a function of the in-plane voltage. The experimental data (a) are qualitatively well reproduced by the profiles calculated with the diffusion model in the presence of an in-plane electric field (b).

and is given by the Maxwell-Boltzmann thermal distribution.²⁶ In the present case this corresponds to assuming that the time needed to thermalize is very short compared to the time scale on which the motion occurs. Although this assumption is not justified *a priori*, we will show below that this diffusion model can describe the experimental data reasonably well both for resonant and nonresonant excitation conditions, and provides a useful tool to determine the transport parameters of excitonic complexes.

A. Determination of the trion mobility

Without an in-plane electric field the steady-state form of Eq. (1) yields

$$D\nabla^2 n(x,y) + I(x,y) - \frac{n(x,y)}{\tau} = 0. \quad (2)$$

In order to compare the experimental results with Eq. (2) we assume that the PL intensity is proportional to $n(x,y)$. Furthermore, we have taken $I(x,y)$ to be proportional to the laser profile. For the lifetime we have used the values measured independently as a function of temperature (for the

300-Å QW, τ varies linearly with temperature, from 177 ps at 4.2 K to 405 ps at 12.5 K).¹² D has been left as a fit parameter. The result for the 300-Å QW at 4.2 K is shown in Fig. 8. The best fit to the data is obtained with $D = 30 \text{ cm}^2 \text{ s}^{-1}$. We observe that for $D = 25 \text{ cm}^2 \text{ s}^{-1}$ and $D = 35 \text{ cm}^2 \text{ s}^{-1}$ the fits start deviating from the experimental data, and therefore we estimate an error $\Delta D = \pm 5 \text{ cm}^2 \text{ s}^{-1}$. The calculated curve describes the data very well down to an intensity of $I = I_{\text{max}}/5$. The model underestimates the PL intensity at larger distances, which is probably due to the assumptions made in the model—i.e., a homogeneous thermal distribution and a constant particle recombination time for all trions, irrespective of their in-plane k vector. A more detailed analysis of the experimental data should use the kinetic Boltzmann equation, avoiding the diffusion approximation.²⁶

However, since the overall agreement between model and experiment is reasonably good, it allows us to estimate the trion diffusion constant and, by means of the Einstein relation $D = \mu e k T$, the trion mobility $\mu = 6.5 \times 10^4 \text{ cm}^2 \text{ V}^{-1} \text{ s}^{-1}$. This value for the mobility can be used to describe the data for the entire temperature range measured. The solid lines in Fig. 4 are the extents calculated with the diffusion model using this value for the mobility and the measured trion lifetimes.¹² To confirm the validity of this estimation we can compare the value with the electron mobility found with transport measurements under nominally the same conditions of electron concentration, $\mu_e = 2 \times 10^5 \text{ cm}^2 \text{ V}^{-1} \text{ s}^{-1}$. Despite the fact that the two values have been found with different experimental techniques, the comparison indicates that the value of μ for X^- is in reasonable agreement with the larger mass of X^- with respect to the electron mass.

Also the experimental results of the 100-Å QW can be described using a constant mobility of $10^4 \text{ cm}^2 \text{ V}^{-1} \text{ s}^{-1}$ (lower solid line in Fig. 4). The lower mobility must be ascribed to the higher disorder in this QW due to the stronger influence of the interface roughness.

B. Trion drift in electric field

The application of an in-plane voltage leads to a direct force on the trions given by $\mathbf{F} = -e\mathbf{E}$, with \mathbf{E} being the electric field.

We have used the steady-state version of Eq. (1) to simulate the data measured at 4.2 K in the presence of an in-plane voltage using the zero-field parameters ($D = 30 \text{ cm}^2 \text{ s}^{-1}$ and $\tau = 177 \text{ ps}$) and varying the electric field. Figure 9 shows the comparison between the experimental data [panel (a)] and the calculated curves [panel (b)]. The electric field has been chosen so to obtain the best agreement with the experimental data. It is clear that the simple diffusion model can describe the variation of the PL profile with the applied voltage very well, which is further confirmation that negative trions behave like free negative quasiparticles drifting in an electric field.

A closer inspection of the calculated curves evidences two interesting points: (i) Similar to the zero-field case, also with an in-plane field, the experimental curves show a more pronounced tail at larger distances compared to the calculated

curves. These results should stimulate further theoretical work to investigate the limits of applicability of the diffusion equation. (ii) The values of the electric field used are one order of magnitude higher than those obtained by simply dividing the applied voltage by the sample length (2 mm, equal to the distance between the source and the drain contacts). The reason for this is not known at present and is the subject of further investigations. Here we will merely discuss two possible causes: namely, a reduced electron density due to the laser illumination and trion drag by electron transport.

Previous investigations have shown that illumination with a laser beam leads to a reduction of the electron density under the laser spot.²¹ A confirmation that this occurs in our experiment is given by the estimation of the Fermi energy of 4.3 meV, from the width of the 2DEG PL spectrum at zero gate voltage (see discussion of Fig. 2). This value is considerably lower than the value found by transport measurements in the same sample $E_F = 5.5 \text{ meV}$,²¹ suggesting that indeed the electron density is locally reduced. A possible consequence is that trions also feel an effective radial electric field, without the application of an in-plane voltage. It is expected that the reduction of the electron density depends on the intensity of the laser light. Investigation of the trion motion as a function of the excitation intensity for no in-plane voltage will further elucidate this issue.

Application of an in-plane electric field leads, apart from a drift force on trions, also to a flow of electrons in the same direction. Taking into account electron-trion scattering, the response of the trions to the field is the combined action of the direct electric force $-e\mathbf{E}$ and the drag force. Our model neglects the drag force and only includes the direct force. As a consequence the measured response of the trion to the field might be larger than that expected from the direct force alone. The drag force heavily depends on the electron transport properties—that is, the conductivity of the QW layer. The direct force instead is independent of the carrier density. The study of trion motion under resonant excitation conditions as a function of the electron density will reveal the effect of the drag force. Furthermore, it will provide a means of studying the electron-trion interactions.

V. EXCITON AND TRION DIFFUSION AFTER NONRESONANT EXCITATION

When both excitons and trions are excited, the diffusive motion of both species should be taken into account, including the transformation from one particle to the other. To describe our nonresonant excitation experiment we have extended Eq. (1) to a system of two coupled diffusion equations:

$$D_X \nabla^2 n_X(x, y) + I(x, y) - n_X(x, y) \left(\frac{1}{\tau_X} + \frac{1}{\tau_{\text{form}}} \right) = 0, \quad (3a)$$

$$D_{X^-} \nabla^2 n_{X^-}(x, y) + \frac{n_X(x, y)}{\tau_{\text{form}}} - \frac{n_{X^-}(x, y)}{\tau_{X^-}} = 0. \quad (3b)$$

Here D_X and D_{X^-} are the diffusion constants for excitons and trions, respectively, τ_X and τ_{X^-} are their respective radiative lifetimes, and τ_{form} is the trion formation time. The lifetimes of the two species have been measured independently¹² at gate voltages for which only X ($\tau_X = 1100$ ps) or X^- ($\tau_{X^-} = 177$ ps) were present in the PL spectrum.

In our description we assume that the photoexcited free electron-hole pairs relax solely to excitons; i.e., the direct formation of trions is neglected.²⁰ Trions are exclusively formed by excitons that capture an extra electron with a characteristic time constant τ_{form} that depends on the electron density. Note that in this model τ_{form} is the only parameter that depends on the electron density. As mentioned above, at 4.2 K the reverse effect—i.e., the dissociation of trions into excitons and free electrons—can be neglected.

Let us first examine the two extreme cases of the coupled equations (3)—that is, low and high gate voltages. For low voltages—i.e., low electron densities—the X^- formation time is very long and much longer than the exciton lifetime. In a first approximation we can neglect the term $1/\tau_{form}$ with respect to $1/\tau_X$ in Eq. (3a). By fitting the measured profile of the exciton PL emission at a gate voltage of -0.78 V we determine $D_X = 120$ cm² s⁻¹. The excitons diffuse for a relatively long distance and locally form trions (see, e.g., bottom panel of Fig. 6).

For high electron concentration ($V = -0.62$ V), the trion formation time is very short and much shorter than the X lifetime. As a consequence the X profile is very narrow and weak (top panel of Fig. 6), as the trion formation is dominant. Since in this regime trion diffusion is relevant, the trion PL profile coincides with the trion profile obtained under resonant excitation conditions (see Fig. 7). We can reproduce this coincidence by putting $\tau_{form} \rightarrow 0$, leading to $n_X \rightarrow 0$, which gives [Eq. (3a)] $I(x, y) = n_X / \tau_{form}$. As a consequence Eq. (3b) becomes equal to Eq. (2), leading to the same profile for resonant and nonresonant excitation.

In the intermediate regime the situation is much more complex. Here the X^- formation time is comparable to the X

radiative lifetime and excitons diffuse until they either recombine or form trions. As a consequence the trion profile is much larger than that measured for resonant excitation (Fig. 7) but is mainly determined by exciton diffusion and subsequent trion formation (see also the results of a similar experiment in the case of CdTe reported in Ref. 19). As a matter of fact, the local ratio between the X and X^- concentration is determined by a dynamical equilibrium between the two species, which depends on the relative values of the characteristic times (τ_X , τ_{X^-} , and τ_{form}).²⁷ Consequently the spatial distributions of X and X^- are quite similar (see panels in Fig. 6 and final results in Fig. 7). A detailed description of these profiles is extremely difficult since the concentration of the two species is *a priori* not homogeneous, which can result in a variation of the characteristic times along the profiles. Moreover, the inhomogeneous illumination is likely to produce a local variation of the electron density, which also affects the value of the X^- formation time.

VI. CONCLUSIONS

We have studied the lateral motion of negative trions in GaAs quantum wells by imaging their spatially and spectrally resolved PL emission after pointlike excitation. We have shown that in high-quality samples trions diffuse from their excitation point and drift in the direction opposite to an applied electric field, demonstrating that they behave as free negative quasiparticles. By a temperature and carrier density-dependent diffusion experiment we have determined the mobility to be as high as $\mu = 6.5 \times 10^4$ cm² V⁻¹ s⁻¹. The same study performed on a sample of lower quality shows a different behavior, consistent with localized trions, or lower mobility $\mu = 10^4$ cm² V⁻¹ s⁻¹.

Studying the motion of excitons and trions after nonresonant excitation of free electron-hole pairs reveals that the spatial distribution of trions is generally determined by the relaxation of moving excitons. Only under very specific conditions of electron concentration is the effect of neutral excitons not important and the trion diffusion can be measured.

*Present address: School of Physics and Astronomy, University of Nottingham, University Park, Nottingham NG7 2RD, United Kingdom. Electronic address: Fabio.Pulizzi@nottingham.ac.uk

†Present address: Department of Physics, University of Sheffield, S3 7RH, United Kingdom.

‡Present address: School of Physics, University of New South Wales, Sydney 2052, Australia.

¹M. Lampert, Phys. Rev. Lett. **1**, 450 (1958).

²K. Kheng, R.T. Cox, Y. Merle d'Aubigné, F. Bassani, K. Saminadayar, and S. Tatarenko, Phys. Rev. Lett. **71**, 1752 (1993).

³A.J. Shields, M. Pepper, D.A. Ritchie, M.Y. Simmons, and G.A.C. Jones, Phys. Rev. B **51**, 18 049 (1995).

⁴A.J. Shields, J.L. Osborne, M.Y. Simmons, M. Pepper, and D.A. Ritchie, Phys. Rev. B **52**, R5523 (1995).

⁵P. Kossacki, J. Cibert, D. Ferrand, Y. Merle d'Aubigné, A. Arnoult, A. Wasiela, S. Tatarenko, and J.A. Gaj, Phys. Rev. B **60**, 16 018 (1999).

⁶H. A. Bethe and E. E. Salpeter, *Quantum Mechanics of One and*

Two Electrons Atoms (Springer, Berlin, 1957).

⁷A.J. Shields, M. Pepper, M.Y. Simmons, and D.A. Ritchie, Phys. Rev. B **52**, 7841 (1995).

⁸M. Hayne, C.L. Jones, R. Bogaerts, C. Riva, A. Usher, F.M. Peeters, F. Herlach, V.V. Moshchalkov, and M. Henini, Phys. Rev. B **59**, 2927 (1999).

⁹D.R. Yakovlev, V.P. Kochereshko, R.A. Suris, H. Schenk, W. Ossau, A. Waag, G. Landwehr, P.C.M. Christianen, and J.C. Maan, Phys. Rev. Lett. **79**, 3974 (1997).

¹⁰G. Finkelstein, H. Shtrikman, and I. Bar-Joseph, Phys. Rev. Lett. **74**, 976 (1995).

¹¹G. Eytan, Y. Yayon, M. Rappaport, H. Shtrikman, and I. Bar-Joseph, Phys. Rev. Lett. **81**, 1666 (1998).

¹²D. Sanvitto, R.A. Hogg, A.J. Shields, D.M. Whittaker, M.Y. Simmons, D.A. Ritchie, and M. Pepper, Phys. Rev. B **62**, 13 294 (2000).

¹³V. Ciulin, P. Kossacki, S. Haacke, J.D. Ganière, B. Deveaud, A. Esser, M. Kutrowski, and T. Wojtowicz, Phys. Rev. B **62**, 16 310

- (2000).
- ¹⁴A. Esser, E. Runge, R. Zimmerman, and W. Langbein, Phys. Rev. B **62**, 8232 (2000).
 - ¹⁵B. Stébé, G. Munsch, L. Stauffer, F. Dujardin, and J. Murat, Phys. Rev. B **56**, 12 454 (1997).
 - ¹⁶D. Sanvitto, F. Pulizzi, A.J. Shields, P.C.M. Christianen, S.N. Holmes, M.Y. Simmons, D.A. Ritchie, J.C. Maan, and M. Pepper, Science **294**, 837 (2001).
 - ¹⁷M.T. Portella-Oberli, V. Ciulin, S. Haacke, J.D. Ganièée, P. Kos-sacki, M. Kutrowski, T. Wojtowicz, and B. Deveaud, Phys. Rev. B **66**, 155305 (2002).
 - ¹⁸H.W. Yoon, A. Ron, M.D. Sturge, and L.N. Pfeiffer, Solid State Commun. **100**, 743 (1996).
 - ¹⁹F. Pulizzi, W.H.A. Thijssen, P.C.M. Christianen, J.C. Maan, D.R. Yakovlev, W. Ossau, T. Wojtowicz, G. Karczewski, and J. Kossut, Physica B **298**, 397 (2001).
 - ²⁰D. Sanvitto, R.A. Hogg, A. Shields, M.Y. Simmons, D.A. Ritchie, and M. Pepper, Phys. Status Solidi B **227**, 297 (2001).
 - ²¹A.J. Shields, J.L. Osborne, M.Y. Simmons, D.A. Ritchie, and M. Pepper, Semicond. Sci. Technol. **11**, 890 (1996).
 - ²²G. Finkelstein, V. Umansky, I. Bar-Joseph, V. Ciulin, S. Haacke, J.D. Ganière, and B. Deveaud, Phys. Rev. B **58**, 12 637 (1998).
 - ²³R.A. Hogg, D. Sanvitto, A.J. Shields, M.Y. Simmons, D.A. Ritchie, and M. Pepper, Physica B **272**, 412 (1999).
 - ²⁴J.G. Tischler, A.S. Bracker, D. Gammon, and D. Park, Phys. Rev. B **66**, 081310 (2002).
 - ²⁵Y. Yayon, A. Esser, M. Rappaport, V. Umansky, H. Shtrikman, and I. Bar-Joseph, Phys. Rev. B **64**, 081308 (2002).
 - ²⁶K. Hess, *Advance Theory of Semiconductor Devices* (Prentice Hall, Englewood Cliffs, NJ, 1988).
 - ²⁷C.R.L.P.N. Jeukens, P.C.M. Christianen, J.C. Maan, D.R. Yakovlev, W. Ossau, V.P. Kochereshko, T. Wojtowicz, G. Karczewski, and J. Kossut, Phys. Rev. B **66**, 235318 (2002).